AIMS Materials Science, 6(4): 610–620.
DOI: 10.3934/matersci.2019.4.610
Received: 20 March 2019
Accepted: 29 May 2019
Published: 08 July 2019

http://www.aimspress.com/journal/Materials

Research article

Synthesis of easily sinterable ceramic electrolytes based on Bi-doped 8YSZ for IT-SOFC applications

Luca Spiridigliozzi[1], Grazia Accardo[2], Emilio Audasso[3], Barbara Bosio[3], Sung Pil Yoon[2] and Gianfranco Dell'Agli[1,*]

[1] Department of Civil and Mechanical Engineering, University of Cassino and Southern Latio, Via G. Biasio 43, 03043 Cassino (FR) Italy
[2] Center of Hydrogen-Fuel Cell Research, Korea Institute of Science and Technology, Hwarangno 14-gil, Seongbuk-gu, Seoul 136-791, South Korea
[3] Department of Civil, Chemical and Environmental Engineering, University of Genova, Via Opera Pia 15, 16145, Genova (GE), Italy

* **Correspondence:** Email: gianfranco.dellagli@unicas.it; Tel: +397762993682; Fax: +397762993711.

Abstract: Ceramic electrolytes formed by Bi (4 mol%)-doped 8YSZ, i.e., Y_2O_3 (8 mol%)-doped ZrO_2, were synthesized by a simple co-precipitation route, using ammonia solution as precipitating agent. The amorphous as-synthesized powders convert into zirconia-based single phase with fluorite structure through a mild calcination step at 500 ℃. The calcined powders were sintered at very low temperatures (i.e., 900–1100 ℃) achieving in both cases very high values of relative densities (i.e., >95%); the corresponding microstructures were highly homogeneous and characterized by micrometric grains or sub-micrometric grains for sintering at 1100 ℃ and 900 ℃, respectively. Very interesting electrochemical properties were determined by Electrochemical Impedance Spectroscopy (EIS) in the best samples. In particular, their total ionic conductivity, recorded at 650 ℃, are 6.06×10^{-2} S/cm and 4.44×10^{-2} S/cm for Bi (4 mol%)-doped 8YSZ sintered at 1100 ℃ and 900 ℃, respectively. Therefore, Bi was proved to be an excellent sintering aid dopant for YSZ, highly improving its densification at lower temperatures while increasing its total ionic conductivity.

Keywords: yttria-doped zirconia; bismuth oxide; co-precipitation; ceramic electrolyte; sintering aids; ionic conductivity

1. Introduction

Solid oxide fuel cells (SOFCs), being able to directly convert chemical energy of hydrocarbon fuels into electricity, are regarded as the next generation of energy conversion devices mainly for them high efficiency, low environmental impact and high fuel flexibility [1]. One of the most important components of a SOFC is the ceramic electrolyte, which must own several challenging properties such as very high ionic conductivity, good mechanical strength and high chemical and thermal stability. The state-of-the-art material that better fulfill these requirements is the fluorite-structured yttria (8 mol%) doped-zirconia (8YSZ), which has been widely applied in a variety of fields, with specific interest as electrolyte in solid oxide fuel cells (SOFC) [2,3]. More recently, it also found application in composites with interesting thermal properties [4] and as porous ceramic material [5,6]. 8YSZ has an adequate ionic conductivity as electrolyte in SOFCs only at temperatures higher than 800 ℃. However, at such high temperatures, high material costs, limited durability and similar drawbacks have been penalizing their commercialization and market diffusion [7]. To this regard, it is imperative to reduce the operating temperature of SOFCs by developing the so-called intermediate temperature SOFC (IT-SOFCs), which have operating temperatures in the range 500–800 ℃; this goal requires the significant increase of the ionic conductivity of the adopted ceramic electrolyte. A first possibility to fulfill this target is to use ceramic electrolytes based on different classes of materials such as doped and/or co-doped ceria [8–10] or the very recently proposed rhombohedral Bismuth oxide [11], whilst a second strategy consists of improving the properties of existing yttria-doped zirconia ceramics by further adding selected dopants [12]. To this regard, several reviews about SOFC materials can be found in literature. Mahato [13] authored a comprehensive review for each SOFC components, electrolyte included. Da Silva [14] reviewed novel materials for SOFC, among them novel oxide ion conductors (e.g., lanthanum apatites and molybdenum oxides), and novel protonic conductors were discussed. The use of additives in 8YSZ has been previously studied mainly because they do not simply improve the final electrochemical properties, but also they lead to a significant reduction of the sintering temperature. In fact, zirconia-based ceramics are usually sintered at about 1600 ℃, thus causing manufacturing difficulties during the production. Among different possible dopants, Bi_2O_3 has been extensively studied for several materials, especially for fluorite phase materials such as doped-ceria [15] and doped-zirconia [2,16], even if some conflicting results are reported in literature [16]. Furthermore, in order to improve the ceramic sinterability, a key point is to dispose of very reactive powders. Various synthesis methods have been proposed in literature to prepare highly reactive zirconia-based nanopowders, such as hydrothermal treatment [17], homogeneous precipitation [18,19], combustion synthesis [20], precipitation [21], sol-gel [22], etc. Due to its intrinsic higher simplicity and lower cost, a series of different samples of Bi (4 mol%)-doped 8YSZ were synthesized via co-precipitation method. The as-synthesized sample was sintered at 900 ℃ and 1100 ℃ and the electrochemical behavior was ascertained by Electrochemical Impedance Spectroscopy. The obtained results highlighted the very positive effect of Bi_2O_3 in the samples both on powders sinterability and on sintered pellets electrochemical properties.

2. Materials and method

2.1. Synthesis of the materials

$ZrO(NO_3)_2$ nH_2O (Sigma-Aldrich, Italy), $Y(NO_3)_3$ $6H_2O$ (Carlo Erba, Italy) and Bi_2O_3 (Carlo Erba, Italy) were used as starting materials without any further purification. Ammonia solution (NH_3 30%, Carlo Erba, Italy) was used as precipitating agent. The co-precipitation was carried out in two separate steps: firstly, two solutions were prepared. The first one (solution A) was obtained by dissolving the proper amount of raw materials in diluted nitric acid (~1 M), in order to have into the solution the following atomic ratio Bi:Y:Zr = 4.0:14.2:81.8, which corresponds to $BiO_{1.5}$ (4 mol%)-8YSZ as global composition. The second one (solution B) was obtained by diluting ammonia solution up to about 4 M. Subsequently, solution B was quickly added to solution A (kept under vigorous stirring), to induce the formation of a white precipitate by using an excess of ammonia solution in order to ensure the completion of the co-precipitation process. The as-obtained sample (even after calcination and sintering) will be labelled as 4Bi-8YSZ in the following. After a short ageing of the suspension (about 10 minutes), the as-obtained co-precipitate was recovered by vacuum filtration, then repeatedly washed with deionized water to remove undesired ions, and finally dried overnight at 70 ℃. A final calcination step in air, at 500 ℃ for 1 h, was carried out to allow the crystallization of the fluorite phase and the complete dissolution into the fluorite lattice of yttrium and bismuth cations.

2.2. Characterization of the materials

The formed phases of the various samples were detected by X-ray Diffraction (XRD) by using a diffractometer (X'PERT, Panalytical, Almelo, The Netherlands) with CuKα radiation. The crystal size of the samples was calculated using the Scherrer formula, whereas the cell parameters of the fluorite phases were calculated by the least-square procedure proposed by Razik [23].

The thermal behavior of the powders was determined by thermogravimetric analysis and differential thermal analysis (DTA-TGA) in air (STA 409 Thermoanalyzer, Netzsch Instruments, Selb, Germany) with a heating rate of 10 ℃·min^{-1} up to 1200 ℃ and using α-Al_2O_3 as a reference.

The calcined powders were formed in a cylindrical shape by uniaxial pressing and finally sintered in air at 900 ℃ and 1100 ℃ by using 5 ℃·min^{-1} as heating rate and 3 h as soaking time. The microstructure of the sintered pellets and of the calcined powders was highlighted by Scanning Electron Microscopy (SEM), using an instrument (Novasem, FEI Co.) equipped with both the standard ETD detector and with EDS microanalysis. The external surfaces of both pellets were polished and to highlight the grain boundaries, a thermal etching for 1 h at a temperature of 100 ℃ lower than the sintering temperature was carried out. The relative density of the sintered pellets was evaluated by hydrostatic balance.

The electrochemical properties have been investigated by EIS technique. The measurements were performed on sintered pellets using a gold conductive paste deposited on both sides of pellets as electrodes. Measurements were carried out in 650–900 ℃ temperature range using a frequency response analyzer (FRA, Solartron 1260) coupled with a dielectric interface (Solartron 1296) in the frequency range 0.1 Hz–1 MHz. The data analysis of measured impedances was carried out using the ZPlot and Zview software.

3. Results and discussion

The 4Bi-8YSZ co-precipitate has an amorphous structure as it clearly appears in the diffraction patterns shown in Figure 1a, displaying only a very broad halo centered at about 30 ° (2θ). The appearance of the diffraction pattern in Figure 1a is the typical one of amorphous co-precipitates of zirconia-based ceramics with ammonia solutions [24,25].

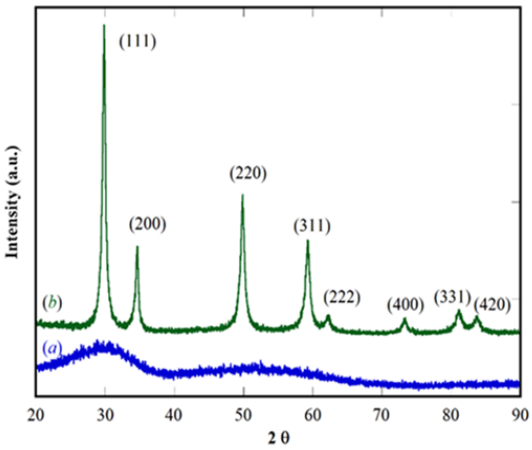

Figure 1. X-ray diffraction patterns of co-precipitated (a) and calcined (b) 4Bi-8YSZ.

The thermal behavior of sample 4Bi-8YSZ is displayed in Figure 2 and it is characterized by a noticeable weight loss (37%), see Figure 2B. Most of this loss is attributable to absorbed water released at low temperature, well highlighted by the large endothermic peak at about 170 ℃ (see Figure 2A) which is almost superimposed to the peak of derivative of weight loss. At higher temperature, the zirconia-based sample crystallizes in the fluorite form, as highlighted by the exothermic peak at 520 ℃. It is interesting to notice that the presence of bismuth in the crystallizing amorphous materials strongly influences the crystallization temperature of cubic zirconia, i.e., by remarkably increasing it of about 50–80 ℃. In fact, amorphous 8YSZ coprecipitated with an analogous process using ammonia solution exhibited the crystallization peak at 445 ℃ when the DTA was carried out in the same conditions, i.e., the same heating rate [3]. In general both pure zirconia and variously doped zirconia (starting from an amorphous phase obtained with analogous precipitation processes) crystallize at around 420–460 ℃ [24,25].

The data reported in Figure 2, considering that DTA-TGA is a dynamic measurement, suggested that a calcination step at 500 ℃ sufficed for completing the thermal decomposition and allowing the crystallization of fluorite structure (we wanted to hold the calcination temperature as low as possible in order to avoid unnecessary grain growth phenomena). The diffraction pattern of the calcined sample displayed in Figure 1b shows only the peaks of fluorite structure zirconia, thus indicating the complete dissolution of yttrium and bismuth in the lattice. The cell parameter of calcined 4Bi-8YSZ and calculated by least-square procedure is 0.5167(2) nm, which is almost coincident with the theoretical value equal to 0.5160 nm. The theoretical *a*-value has been estimated starting from the nominal composition of sample 4Bi-8YSZ and using the following correlation to evaluate the lattice parameter for fluorite structures based on ZrO_2 proposed by Kim [26]:

$$a = 0.5120 + \sum_i (0.0212\Delta r_i + 0.00023\Delta z_i)m_i \quad (1)$$

where a is the cell parameter (in nm) of the fluorite oxide at room temperature, Δr_i is the difference between the ionic radius of the dopant ions (i.e., Y and Bi) and Zr^{4+} in 8-fold coordination, Δz_i is the difference in charge between the dopants and Zr^{4+}, and m_i is the concentration of ith dopant expressed as mole percentage in the form of MO_x.

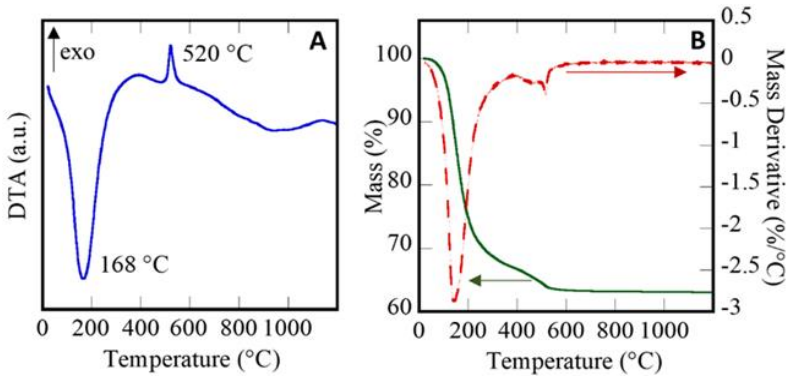

Figure 2. DTA (A) and TGA (solid green line) and derivative of TGA (dotted red line) of coprecipitated 4Bi-8YSZ (B).

On the contrary, the cell parameter of sample 4Bi-8YSZ is rather higher than the theoretical value of 8YSZ, equal to 0.5139 nm (see ICDD n. 30-1468), signaling again the substitution of Y^{3+} and Zr^{4+} with larger cations, as Bi^{3+}. Therefore, we can assume that calcined 4Bi-8YSZ is constituted by a single phase with fluorite structure in which the cations are Zr^{4+}, Y^{3+} and Bi^{3+}. The crystal size, determined by Scherrer formula using the main XRD peak (111), is 18 nm so proving the very low crystal growth resulting from the calcination step. Despite the very low crystal size, the morphology of the calcined powders is characterized by much larger particles with irregular shape (see Figure 3). The big particles are actually clusters of rounded sub-micrometric particles (highlighted in the inset in Figure 3). Indeed such morphology is frequently observed in powders of calcined zirconia based materials obtained from wet-chemical method [3].

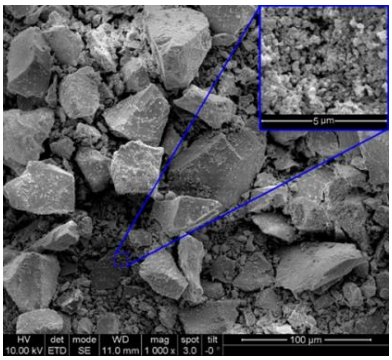

Figure 3. SEM micrographs of 4Bi-8YSZ calcined at 500 ℃ for 1 h, at lower and higher (inset) magnification.

The calcined powders were pressed by uniaxial pressing and then sintered at two different temperatures, 900 ℃ and 1100 ℃. The final relative densities of the samples were measured through Archimede's principles by using a hydrostatic balance and resulted to be 96.5%, for the sintering at 900 ℃, and 98.6% for the sintering at 1100 ℃, thus showing very good densification despite the far from ideal morphology of the calcined powders and the low sintering temperature. This suggests that the presence of Bi was able to substantially reduce the sintering temperature. The microstructures of both the pellets, obtained by SEM analysis, are displayed in Figure 4. At a first glance both the microstructures are very dense, according with the very high relative density, and quite homogeneous, with the presence of regular and equiaxed grains. The sample sintered at 900 ℃ exhibits very small grains, whose size is in the order of several hundreds of nanometers, and some residual porosity (Figure 4a). Despite the rather low sintering temperature, the microstructure highlighted in Figure 4a remains certainly adequate for use as SOFC electrolyte. However, the sample sintered at 1100 ℃, is characterized by an even denser texture highlighted by the practical absence of any porosity (see Figure 4b) confirming the measured density next to 99%. The grain size is in the order of some micrometers and it is obviously well larger than the one of the pellet sintered at 900 ℃.

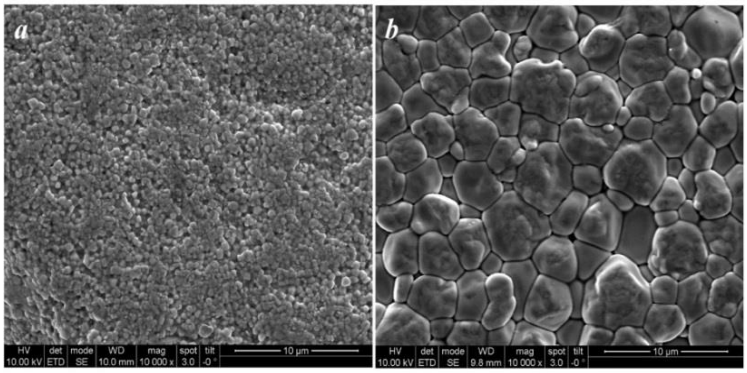

Figure 4. SEM micrographs of 4Bi-8YSZ sintered at 900 ℃ for 3h (a) and at 1100 ℃ for 3h (b).

In order to evaluate the amount of Bi present in the samples and its distribution, the EDS analysis was carried out on the pellets. The cationic composition obtained from the whole area shown in Figure 5 (related to the sample sintered at 1100 ℃) is Bi = 4%, Y = 18% and Zr = 78%. These values are in good agreement with the nominal composition reported in materials and methods section. Therefore, these results support the previous evaluations based on XRD data and consequently we can claim that zirconia co-doped with yttrium and bismuth can be prepared by co-precipitation with ammonia. Furthermore, Figure 5 presents a homogeneous distribution of bismuth, as shown by the fuchsia dots. Bi is present both inside the grains and in the grain boundaries, and only in very few of the latter a slightly excess is registered.

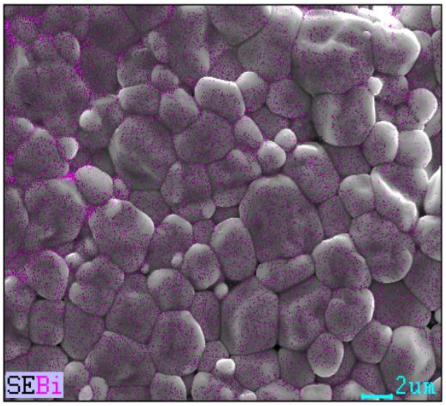

Figure 5. EDS mapping of Bi for sample sintered at 1100 ℃ for 3 h.

To detect possible phase-stability issues as a consequence of the sintering, X-ray analysis was carried out on the sample sintered at 1100 ℃, after grinding by hand [27]. The related diffraction pattern is displayed in Figure 6. It is clear that only peaks belonging to fluorite-like cubic zirconia are present, with the exception of just some perceivable peaks (marked with a star), that can be ascribed to a negligible amount of monoclinic zirconia. Thus, no significant phase modification occurred during the sintering treatment, and the fluorite-like structure of 4Bi-8YSZ is expected to be definitely stable at the IT-SOFCs operating conditions.

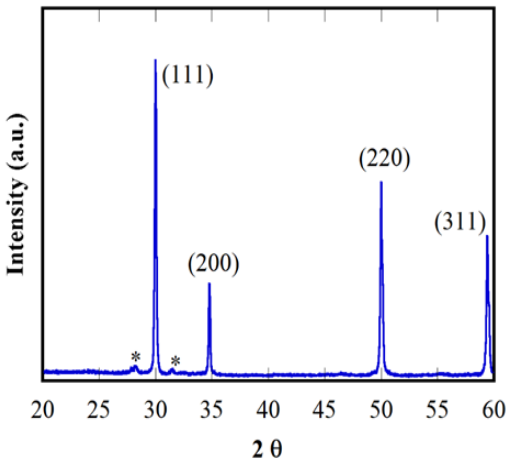

Figure 6. X-ray diffraction patterns of 4Bi-8YSZ sintered at 1100 ℃ for 3 h.

Finally, both sintered pellets were characterized by EIS in order to investigate their electrochemical properties. The measured data have been fitted using an equivalent circuit, consisting of two (R-CPE) elements joined together in series representing the total (bulk + grain boundary) contribution (Rt-CPE) and the electrode contribution (Rel-CPE), to estimate the total resistivity values [28]. In the analyzed temperature range (i.e., 650–900 ℃) all Nyquist plots exhibit a large semicircle due to the electrodes process and a smaller faint semicircle in the high-frequency region corresponding to the whole electrolyte process. The two separated contributions of bulk and grain boundary could not be separately detected. This is due to the high temperature that weakens their

response causing them to assume frequencies beyond the range of investigation [29]. In the Nyquist plot in Figure 7, the best-sintered sample (1100 ℃) is shown as representative highlighting the impedance behavior at 650 ℃ along with the rather good accordance between measured and fitted data.

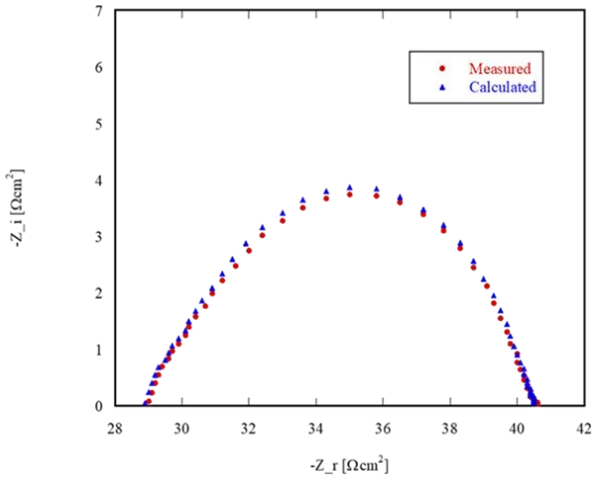

Figure 7. Nyquist plot at 650 ℃ of 4Bi-8YSZ sintered at 1100 ℃.

All the data collected in the range 650–900 ℃, for both the sintered samples, were summarized in the Arrhenius plots shown in Figure 8. In the analyzed temperature range, a nearly perfect linear trend for both samples appears. The electrochemical properties achieved for 4Bi-8YSZ samples are better than the ones of conventional 8YSZ electrolytes sintered in the temperature range of 1300–1650 ℃ [16]. In particular, the total ionic conductivity, recorded at 650 ℃, is 6.06×10^{-2} S/cm and 4.44×10^{-2} S/cm for 4BiYSZ sintered at 1100 ℃ and 900 ℃, respectively. The higher ionic conductivity of the sample sintered at 1100 ℃ obviously depends on its slightly better microstructural features compared to the ones sintered at lower temperature.

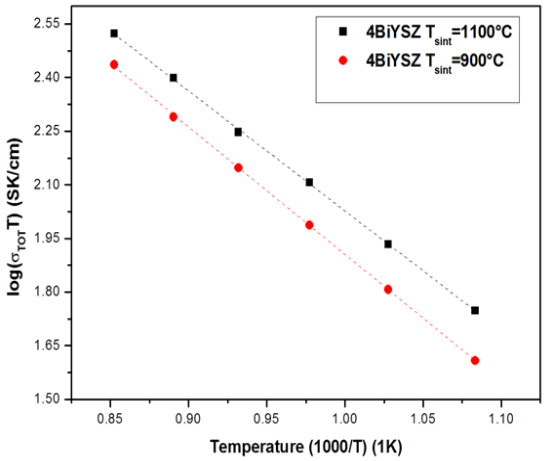

Figure 8. Arrhenius plot of 4Bi-8YSZ, both sintered at 900 ℃ and 1100 ℃.

4. Conclusion

By using a simple and cheap co-precipitation synthesis route, it has been possible to produce very well densified 4Bi-8YSZ pellets in which Bi is homogeneously distributed in the matrix. Bi has been proved to have very positive effects upon sintering behavior, i.e., lowering the sintering temperature of YSZ well below their typical values despite the morphology of the calcined powders far from ideal, favoring enhanced ionic conduction respect to 8YSZ, too. Furthermore, under sintering step the samples do not withstand any phase modification. In conclusion, although further investigations upon synthesis and sintering parameters have still to be done, 4Bi-8YSZ can be considered as a high-performance class of zirconia-based electrolyte for future IT-SOFCs production.

Acknowledgments

This work was supported by KRF—Korea Research Fellowship through the National Research Foundation of Korea and funded by the Ministry of Science, ICT and Future Planning of Republic of Korea (Grant Number 2016H1D3A1908428).

Conflict of interests

The authors declare no conflict of interests.

References

1. Panthi D, Tsutsumi A (2014) Micro-tubular solid oxide fuel cell based on a porous yttria-stabilized zirconia support. *Sci Rep* 4: 5754.
2. Nagao M, Kobayashi K, Hibino T (2014) Low-temperature sintering of yttria-stabilized zirconia using bismuth-vanadium oxide as a sintering aid at 800 ℃. *Chem Lett* 43: 1887–1889.
3. Dell'Agli G, Mascolo G (2003) Sinterability of 8Y-ZrO_2 powders hydrothermally synthesized at low temperature. *Solid State Ionics* 160: 363–371.
4. Barad C, Shekel G, Shandalov M, et al. (2017) Internal nano voids in yttria stabilized zirconia (YSZ) powder. *Materials* 10: 1440.
5. Shekel G, Barad C, Hayun H, et al. (2018) Applying the general effective media (GEM) approach for analyzing the thermal conductivity of ZrO_2-8YSZ composites. *Phys Chem Chem Phys* 20: 16666–16672.
6. Barad C, Shamir D, Cahana M, et al. (2019) Influence of galia (Ga_2O_3) addition on the phase evolution and grain growth behavior of voided yttria stabilized zirconia (YSZ) powder. *J Alloy Compd* 783: 286–291.
7. Joh DW, Park JH, Kim D, et al. (2017) Functionally graded bismuth oxide/zirconia bilayer electrolytes for high performance intermediate-temperature solid oxide fuel cells (IT-SOFCs) *ACS Appl Mater Inter* 9: 8443–8449.
8. Spiridigliozzi L, Dell'Agli G, Biesuz M, et al. (2016) Effect of the precipitating agent on the synthesis and sintering behavior of 20 mol Sm-doped ceria. *Adv Mater Sci Eng* 2016: 6096123.

9. Dell'Agli G, Spiridigliozzi L, Pansini M, et al. (2018) Effect of the carbonate environment on morphology and sintering behaviour of variously co-doped (Ca, Sr, Er, Pr) Samarium-doped Ceria in co-precipitation/hydrothermal synthesis. *Ceram Int* 44: 17935–17944.
10. Jaiswala N, Tanwar K, Suman R, et al. (2019) A brief review on ceria based solid electrolytes for solid oxide fuel cells. *J Alloy Compd* 781: 984–1005.
11. Jolley AG, Jayathilake R, Wachsman ED (2019) Optimizing rhombohedral Bi_2O_3 conductivity for low temperature SOFC electrolytes. *Ionics* 2019: 1–6.
12. Flegler AJ, Burye TE, Yang Q, et al. (2014) Cubic yttria stabilized zirconia sintering additive impacts: a comparative study. *Ceram Int* 40: 16323–16335.
13. Mahato N, Banerjee A, Gupta A, et al. (2015) Progress in material selection for solid oxide fuel cell technology: a review. *Prog Mater Sci* 72: 141–337.
14. Da SFS, De STM (2017) Novel materials for solid oxide fuel cell technologies: a literature review. *Int J Hydrogen Energ* 42: 26020–26036.
15. Accardo G, Frattini D, Ham HC, et al. (2018) Improved microstructure and sintering temperature of bismuth nano-doped GDC powders synthesized by direct sol-gel combustion. *Ceram Int* 44: 3800–3809.
16. Liu L, Zhou Z, Tian H, et al. (2016) Effect of bismuth oxide on the microstructure and electrical conductivity of yttria stabilized zirconia. *Sensors* 16: 369–379.
17. Dell'Agli G, Mascolo G, Mascolo MC, et al. (2005) Crystallization-stabilization mechanism of yttria-doped zirconia by hydrothermal treatment of mechanical mixtures of zirconia xerogel and crystalline yttria. *J Cryst Growth* 280: 255–265.
18. Akhtar K, Haq IU, Hira U (2013) Synthesis and characterization of uniform zirconia particles by homogeneous precipitation method. *High Temp Mat Pr* 32: 391–395.
19. Accardo G, Dell'Agli G, Frattini D, et al. (2017) Electrical behaviour and microstructural characterization of magnesia co-doped ScSZ nanopowders synthesized by urea co-precipitation. *Chem Eng T* 57: 1345–1350.
20. Da Silva CA, Ribeiro NFP, Souza MMVM (2009) Effect of the fuel type on the synthesis of yttria stabilized zirconia by combustion method. *Ceram Int* 35: 3441–3446.
21. Ghahfarokhi SS, Mamoory RS, Kalashami AG (2018) Inverse precipitation synthesis of ZrO_2 nanopowder and in-situ coating on MWCNTs. *Ceram Int* 44: 13556–13564.
22. Barad C, Kimmel G, Hayun H, et al. (2018) Influence of galia (Ga_2O_3) addition on phase transitions and crystal growth of zirconia (ZrO_2). *J Mater Sci* 53: 12741–12749.
23. Razik NA (1985) Precise lattice constants determination of cubic crystals from x-ray powder diffractometric measurements. *Appl Phys A-Mater* 37: 187–189.
24. Dell'Agli G, Mascolo G, Mascolo MC, et al. (2008) Drying effect on thermal behaviour and structural modification of hydrous zirconia gel. *J Am Ceram Soc* 91: 3375–3379.
25. Dell'Agli G, Mascolo G, Mascolo MC, et al. (2006) Weakly-agglomerated nanocrystalline $(ZrO_2)_{0.9}(Yb_2O_3)_{0.1}$ powders hydrothermally synthesized at low temperature. *Solid State Sci* 8: 1046–1050.
26. Kim DJ (1989) Lattice parameters, ionic conductivities, and solubility limits in fluorite-structure MO_2 oxide (M = Hf^{4+}, Zr^{4+}, Ce^{4+}, Th^{4+}, U^{4+}) solid solutions. *J Am Ceram Soc* 72: 1415–1421.
27. Andini S, Montagnaro F, Santoro L, et al. (2018) Mechanochemical processing of blast furnace slag for its reuse as adsorbent. *Chem Eng T* 32: 2299–2304.

28. Frattini D, Accardo G, Moreno A, et al. (2017) A novel nickel-aluminum alloy with titanium for improved anode performance and properties in molten carbonate fuel cells. *J Power Sources* 352: 90–98.
29. Spiridigliozzi L, Dell'Agli G, Marocco A, et al. (2018) Engineered co-precipitation chemistry with ammonium carbonate for scalable synthesis and sintering of improved $Sm_{0.2}Ce_{0.8}O_{1.90}$ and $Gd_{0.16}Pr_{0.04}Ce_{0.8}O_{1.90}$ electrolytes for IT-SOFCs. *J Ind Eng Chem* 59: 17–27.

AIMS Press

© 2019 the Author(s), licensee AIMS Press. This is an open access article distributed under the terms of the Creative Commons Attribution License (http://creativecommons.org/licenses/by/4.0)